Neutron Scattering Study of the Dynamics of Hydronium Ion in $(H_3O)Zr_2(PO_4)_3$ Nasicon Across the Order−Disorder Transition

L. E. Bove,[†] M. Catti,[‡] A. Paciaroni,[†] and F. Sacchetti[†]

Istituto Nazionale per la Fisica della Materia, Unità di Perugia, Dipartimento di Fisica, Università di Perugia, Via A. Pascoli, I-06123 Perugia, Italy, and Dipartimento di Scienza dei Materiali, Università di Milano Bicocca, via Cozzi 53, I-20125 Milano, Italy

Received: November 13, 2003; In Final Form: April 26, 2004

Neutron incoherent scattering measurements were performed on $(H_3O)Zr_2(PO_4)_3$ Nasicon by the quasi-elastic spectrometer IN13 (ILL, Grenoble), to characterize the slow proton dynamics of the H_3O^+ ion in this compound. Both quasi-elastic and elastic data were collected at temperatures above and below the order−disorder phase transition ($T_c = 177$ K). Quasi-elastic contributions with peak full widths at half-maximum of 12 and 33 μeV (corresponding to proton jumping times of 110 and 40 ps) were determined at 150 and 200 K, respectively. This supports a confined proton motion both above (faster) and below (slower) the transition temperature, consistent with the full and partial disorder of the hydronium ion found in the high-*T* rhombohedral and low-*T* monoclinic phase, respectively, by previous neutron diffraction experiments. Results of the elastic scans vs momentum transfer and temperature are analyzed and discussed.

1. Introduction

Nasicon systems, with the simplest composition $AM_2(PO_4)_3$, are well-known for the high mobility therein usually shown by the alkali atoms A, leading to possible applications as solid electrolytes and cathode intercalation materials in electrochemical devices. In particular, the crystal structure of lithium phases such as $LiZr_2(PO_4)_3$ was thoroughly investigated by neutron diffraction, so as to clarify the complex order−disorder of Li atoms and its relation with the polymorphism and ion conduction properties of this material.[1,2] Substitutions of A with ammonium or hydrogen ions were early attempted, producing among others the phase $(H_3O)Zr_2(PO_4)_3$: this showed an electrical conductivity increasing from 5×10^{-7} to 5×10^{-5} Ω^{-1} cm^{-1} in the thermal range 40−160 °C, before dehydration occurred.[3] This conductivity is low for direct applications as proton conductors, but by bonding and pelletizing techniques, a patented product based on hydronium Nasicon, Hyceram, could be prepared and characterized.[4] Besides, there is a clear interest in elucidating the structural and dynamical behavior of H atoms in this phase, to suggest atomistic mechanisms for the process of proton transfer in ionic conductivity.

The presence of the H_3O^+ molecular unit (hydronium ion) in the structure of hydrogenated Nasicon was proved by neutron diffraction,[5,6] thus showing $(H_3O)Zr_2(PO_4)_3$ to be one of the very few solid compounds where this ionic molecular species has been observed. Other examples well characterized by neutron diffraction refer to H_3O^+ in zeolitic frameworks.[7,8] On the other hand, the hydronium ion is quite common in liquid acidic water solutions and is likely to play an important role in complex biological systems, but of course, it is more difficult to characterize structurally and dynamically because of the absence of long-range order. Further, by the recent neutron diffraction study of $(H_3O)Zr_2(PO_4)_3$ an order−disorder phase transition was discovered[6] at $T_c = 177$ K, relating the rhombohedral room-temperature modification (HT) to a monoclinic low temperature (LT) phase. In the HT case, the hydronium ion has pyramidal geometry similar to that observed in zeolite X,[7] but with the O atom lying on a site with $\bar{3}$ rather than 3 symmetry, so as to appear disordered between two states related by an umbrella-like inversion in the symmetry-constrained average structure. The layout of the six hydrogen sites around the O atom of the H_3O^+ ion, which are populated with a $^1/_2$ statistical factor, is shown in Figure 1. In the LT phase, on the other hand, an ordered configuration of H_3O^+ is attained with nearly planar geometry resembling that observed in HSAPO-34 zeolite;[8] however, some residual disorder appears to involve one of the three H atoms, which would flip between two close positions on either side of the H_2O molecular plane.

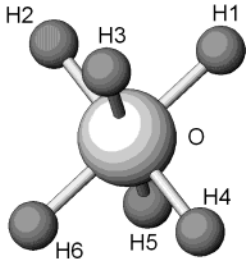

Figure 1. Arrangement of available hydrogen sites in the disordered configuration of the H_3O^+ ion in the HT phase.[6]

As several alternative hydrogen sites are present in $(H_3O)Zr_2(PO_4)_3$, this relatively simple system is also a good prototype for studying the proton dynamics in a multiple potential well. Such dynamical effects in simple crystalline compounds can be very relevant for other fields, too, where a much more complex arrangement of hydrogen bonds exist, like the large and complicated molecules important for biophysics. Indeed, the occupancy distribution of the various hydrogen sites may be static, according to a domain pattern configuration of the crystal, and transitions between different patterns (equivalent to movements of domain walls) would be switched by an

[†] INFM and University of Perugia.
[‡] University of Milano Bicocca.

10.1021/jp037463m CCC: $27.50
Published on Web 05/28/2004

external perturbation, like the sample temperature. On the other hand, the hydrogen distribution observed in the average disordered structure can be due to a dynamic process, and in this case the protons would not occupy the same site all the time. The coherent elastic (diffraction) experiment is not able to discriminate between these two different explanations of disorder, so that other neutron scattering techniques have to be employed to probe directly the dynamical behavior of hydrogen atoms.

Other very interesting and subtle aspects of proton dynamics have been recently revealed, by neutron scattering experiments, in the prototype crystalline system $KHCO_3$, where multiple sites could be available for the H atoms.[9,10] Indeed, in that case an ordered configuration was detected, but parallely the new phenomenon of macroscopic quantum coherence was claimed to be present. This would be related to the fermion behavior of protons and to the ensuing antisymmetric character of their vibrational wave function and would affect both the dynamics and the statics of hydrogen atoms, as they are probed in neutron scattering experiments. A complex behavior of neutron Compton scattering is also observed in KH_2PO_4 and attributed to quantum tunneling.[11] There are thus a number of fundamental studies in progress on the dynamics of protons in simple crystalline systems, which presently make this topic a relevant one in the field of solid-state research.

Therefore, we started an investigation of the slow hydrogen dynamics in $(H_3O)Zr_2(PO_4)_3$ by quasi-elastic and elastic incoherent neutron scattering, with the aim of extracting all possible information about the nature of the proton motion below and above the order−disorder transition temperature, so as to throw light onto the real character of disorder of the hydronium ion in this compound.

2. Experimental Section

The strong incoherent scattering cross section of the proton makes the incoherent neutron scattering a very powerful mean to follow the dynamics of single protons in hydrogen containing systems. As the probe used has a strictly local character, the dynamical behavior seen is quite uncoupled from crystal long-range order effects. The motion of hydrogen between equivalent sites in NASICON can be expected to be rather slow and in the range of several tenths of a picosecond. Therefore, an investigation of such a slow proton dynamics needs high-resolution inelastic neutron scattering experiments in the microelectronvolts (quasi-elastic) energy range. Further, due to the small bond lengths of hydrogen atoms, an extended momentum transfer range should be explored in reciprocal space, to have sensitivity to the motion of protons across short distances of the order of 1 Å. The spectrometer IN13, installed at the High Flux Reactor of the Institut Laue Langevin (Grenoble, France), was found to be very well suited for this investigation because the energy resolution is 9 μeV and a wavevector Q transfer up to 5.3 $Å^{-1}$ is available, with a resolution of about 0.2 $Å^{-1}$.

Two different experiments were performed. The first one was a quasi-elastic experiment, where the final neutron energy was held fixed and the incoming energy was varied in an energy window from −25 to +25 μeV. As the quasi-elastic experiment is very time-consuming, this investigation had to be limited to two temperature values (150 and 200 K) below and above the order−disorder phase transition, respectively. The second experiment was carried out in the elastic configuration, to collect the intensity of the nominally elastically scattered neutrons as a function of the wavevector transfer Q. The elastic scans were performed in a temperature range from 20 to 270 K. In both experiments the sample, which was in the form of a very fine powder,[6] was contained in the space between two thin coaxial aluminum cylinders with radii 20 and 19 mm. In this way the sample geometry was optimized for collecting the scattered neutrons in all directions with minimum difference in the scattering geometry, still having a small sample thickness (1 mm); further, the sample was immersed in the full incoming neutron beam. The sample density, after slightly pressing the powder, was about one-third that of the bulk sample.

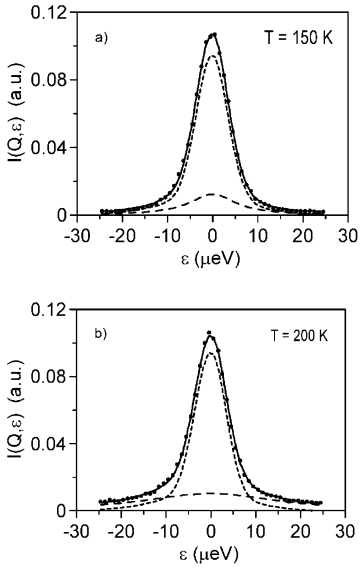

Figure 2. Quasi-elastic experimental intensity (dots) vs energy, compared to the fitting function of eq 1 (full line): (a) results at 150 K; (b) results at 200 K. Short- and long-dashed lines represent the elastic and quasi-elastic components of the intensity, respectively.

The collected data were first corrected for incident flux, cell scattering and self-shielding, and they were eventually normalized with respect to results obtained for a vanadium sample, which was used as a standard isotropic elastic scatterer. No multiple scattering correction was applied, as the scattering power of the present sample turned out to be rather small.

3. Results and Discussion

3.1. Quasi-elastic Scattering Data. The present quasi-elastic results can be analyzed in terms of two components according to the following equation:

$$I_{\mathrm{meas}}(Q,\epsilon) = \int R(\epsilon-\epsilon')\, I_{\mathrm{fit}}(Q,\epsilon')\, \mathrm{d}\epsilon' \qquad (1)$$

where Q and ϵ are the momentum and energy transfers and $R(\epsilon)$ is the instrument energy resolution function as determined from the vanadium scan. In eq 1 the fitting intensity $I_{\mathrm{fit}}(Q,\epsilon)$ is assumed to be contributed by the sum of an elastic ($\epsilon = 0$) and an inelastic component, and in the limit of the present experimental resolution, it can be expressed as

$$I_{\mathrm{fit}}(Q,\epsilon) = \exp[-2W(Q)]a_{\mathrm{e}}(Q)\delta(\epsilon) + a_{\mathrm{qe}}(Q)\frac{1}{\pi}\frac{\Gamma(Q)}{\epsilon^2+\Gamma^2(Q)} \qquad (2)$$

where $\exp[-2W(Q)]$ is the Debye−Waller factor, $a_{\mathrm{e}}(Q)$ is the amplitude of the elastic component, $a_{\mathrm{qe}}(Q)$ and $\Gamma(Q)$ are the amplitude and the half-width at half-height, respectively, of the quasi-elastic contribution; $\delta(\epsilon)$ is 1 for $\epsilon = 0$, and 0 for $\epsilon \neq 0$. Equations 1 and 2 turned out to be quite adequate to fit the experimental data at 150 and 200 K (Figure 2), by optimizing

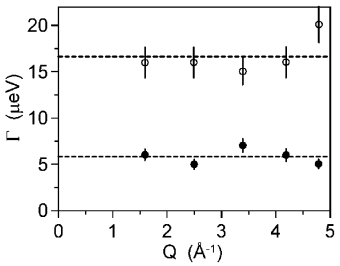

Figure 3. Half-width at half-maximum of the quasi-elastic scattering peak $\Gamma(Q)$ at 150 K (full circles) and 200 K (open circles) as a function of momentum transfer Q. The dashed lines represent the average value at each temperature.

the four parameters $W(Q)$, $a_e(Q)$, $a_{qe}(Q)$, and $\Gamma(Q)$. In Figure 3 we report the half-widths $\Gamma(Q)$ at 150 and 200 K as functions of the momentum transfer Q. To improve the statistics, the detectors were binned in groups of six. However, this binning does not affect the quality of the fitting, as the width Γ of the quasi-elastic term is almost independent of Q, as apparent from Figure 3.

At the lower temperature (150 K), the diffraction results[6] indicate that the system is in a partially ordered state, with two of the three protons located in well-defined sites, but that some residual disorder affects the third proton of the hydronium ion. Indeed, a finite quasi-elastic contribution with a width significantly exceeding that of the instrument resolution appears clearly from the present incoherent scattering data. This demonstrates that there is a residual proton dynamics with a half-width at half-maximum of 5.8 ± 0.5 μeV, consistent with the possible flipping motion of one of the three protons between two sites suggested by the diffraction experiment. At the higher temperature (200 K) a much faster proton dynamics is observed, due to the larger width of 16.5 ± 1.0 μeV; this would correspond to the umbrella-like inversion of the hydronium ion, giving rise to the extensive disorder present in the HT phase.

Therefore, such results suggest that the order−disorder transition is probably connected to the proton dynamics. At low temperature and with slow proton fluctuations, the system would tend to order the protons according to a fixed configuration of the H_3O^+ ion, except for a possible residual flipping motion of one H atom. On increasing temperature, the much faster proton motion would introduce an extensive disorder with six equivalently populated proton sites. The temperature dependence of the quasi-elastic width, on the basis of the two data at 150 and 200 K, is compatible with an Arrhenius trend with activation energy of 55 meV (see below). Measurements at many more temperature values would be needed, of course, to establish the Arrhenius behavior of $\Gamma(T)$ unambiguously.

As the width of the quasi-elastic peak is not Q dependent either below or above T_c, the proton dynamics should be confined in both cases. The mean residence time between subsequent jumps of the proton in its confined potential well is thus simply $\tau = \hbar/\Gamma$, and values of 110 ± 10 and 40 ± 3 ps are derived for τ at 150 and 200 K, respectively. Long-range diffusion of the proton should therefore be excluded on the basis of the present data. Indeed, such a process would produce a peak half-width behavior of type:

$$\Gamma = \hbar DQ^2/(1 + \tau DQ^2) \qquad (3)$$

where D is the diffusion coefficient of the proton. This $\Gamma(Q)$ function has asymptotic behaviors $\Gamma \sim \hbar/\tau$ for $Q \gg 1/\sqrt{(\tau D)}$, and $\Gamma \sim \hbar DQ^2$ (classical diffusion regime) for $Q \ll 1/\sqrt{(\tau D)}$. Thus, one could argue that the observed independence of Γ of Q (Figure 3) may be due to having explored an insufficiently low Q range in the experiment. To prove that this hypothesis is not true, let us consider the 200 K data with an asymptotical $\hbar/\tau$ value of 16.5 μeV: only with D values larger than 10^{-6} cm^2 s^{-1} would the range $\Gamma \sim \hbar DQ^2$ fall below the minimum $Q = 1.5$ Å^{-1} considered in the measurements. Such a D value is unrealistically close to the diffusion coefficient of liquid water (2×10^{-5} cm^2 s^{-1}), whereas, by applying the Nernst−Einstein equation to the ionic conductivity of $(H_3O)Zr_2(PO_4)_3$ measured at room temperature[3,12] one obtains $D \approx 10^{-11}$ to 10^{-12} cm^2 s^{-1}, and values of D measured also by other techniques (e.g., NMR) on solid protonic conductors usually do not exceed 10^{-9} cm^2 s^{-1}.[13] This upper limit for D would correspond to a diffusion regime active for $Q < 30$ Å^{-1}. Therefore, the graph of $\Gamma(Q)$ in Figure 3 should deviate from a constant value well inside the Q range explored, if eq 3 were to be applied as in the case of not-confined proton diffusion.

3.2. Elastic Scattering Data. Additional information can be obtained by analyzing the elastic scattering scans, which, however, are not rigorously elastic, as all scattered neutrons within the instrumental energy resolution width are collected. Therefore, at low temperature, where the width of the quasi-elastic peak becomes small enough, both the elastic and quasi-elastic components can be expected to be included in the nominally ($\epsilon = 0$) elastic intensity. On the other hand, at high temperature the quasi-elastic component is sufficiently broad to come almost completely outside of the nominally elastic scan. Thus, the intensity of the elastic scan is a measure of the quasi-elastic fraction left out of the instrumental energy resolution peak.

The experimental elastic intensity at fixed Q shows, as a function of temperature, a smooth decreasing trend at $T \ll T_c$, but on approaching the transition temperature, it drops suddenly. Of course a nonnegligible fraction of the intensity decrease should come from the hydrogen Debye−Waller factor $\exp[-2W(Q)]$, which is quite high due to the small hydrogen mass.[6] Therefore, we corrected the temperature dependence of the elastic intensity by an appropriate Debye−Waller factor derived from the data themselves. To obtain the temperature dependence of $W(Q)$, a simple Debye model was used with $T_D = 200$ K. Considering the experimental errors, the resulting $W(Q)$ value is in agreement with that one can derive from the diffraction experiment of ref 6. The so corrected data show a substantially constant trend up to about 150 K, followed by an abrupt decrease up to 180 K and again a constant trend at higher temperature. The same behavior is observed qualitatively for all Q values included in the experiment; therefore, at first the data were averaged over all the momentum transfer range and then analyzed.

To enhance the trend in the neighborhood of T_c, we defined the following normalized quantity:

$$S(T) = \frac{I(T) - I_{HT}}{I_{LT} - I_{HT}} \qquad (4)$$

where I_{LT} and I_{HT} are the Debye−Waller corrected intensities at low and high temperature, respectively, in the regions far from T_c, where there is almost no T dependence. The function $S(T)$ is a sort of order parameter of the transition as observed by means of elastic scattering, and it is plotted in Figure 4. Therein the trend of $S(T)$ is also compared to that of the monoclinic unit-cell edge a derived from the diffraction measurements versus T,[6] and a strong similarity is apparent. The jump of $S(T)$ observed at about 175 K agrees nicely with

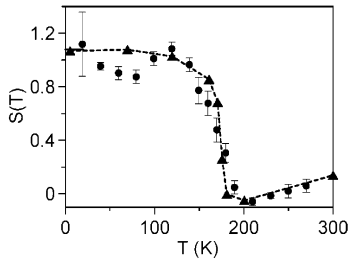

Figure 4. Normalized elastic intensity $S(T)$ (full circles, cf. eq 4) as a function of temperature, compared to the normalized monoclinic unit-cell edge a (triangles) from ref 6.

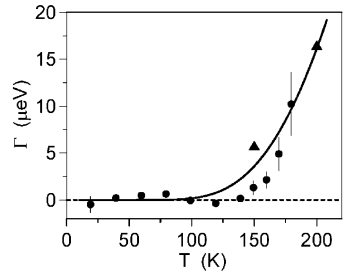

Figure 5. Half-width at half-maximum $\Gamma(T)$ of the quasi-elastic peak (full circles), derived from eq 5 as described in the text, as a function of temperature. Triangles are direct results from the two quasi-elastic scans, and the full line is the Arrhenius plot which fits the whole set of data.

the T_c value determined by the corresponding jumps of unit-cell parameters, confirming that the same process is observed in both the coherent and incoherent elastic scattering experiments.

An approximate analysis of the data of eq 4 can be performed in terms of the width of the quasi-elastic process and the width of the resolution function. By convoluting a Lorentzian quasi-elastic peak with a rectangular approximation of the energy resolution function in an elastic window scan, the following analytic relationship is obtained:

$$S(T) = \frac{2}{\pi}\tan^{-1}\left(\frac{\sigma_R}{\Gamma}\right) \qquad (5)$$

where σ_R is the half-width of the resolution function. By use of eq 5, Γ could be derived directly from the measured $S(T)$. We have checked that a numerical integration using the experimental resolution function provides results that are very similar to those of eq 5. Therefore, this formula was used as a simple analytic approach to estimate the effective peak widths, as determined from the elastic intensity. The results so obtained are shown in Figure 5 as full circles, together with the two peak widths derived from the quasi-elastic scans (triangles). An Arrhenius plot fitting the whole set of data is also displayed, with a characteristic temperature of 900 K (~80 meV activation energy), which corresponds to what was expected for the thermally activated proton jumping. The agreement between the two sets of results appears to be satisfactory, in view of the various approximations and of the quality of the available data.

In addition to the trend of the elastic intensity as a function of temperature, also the Q dependence of the intensity below and above the transition temperature should be analyzed. There are indeed two temperature regions, below 100 K and above 200 K, where the intensity corrected for the Debye−Waller factor is almost constant. In Figure 6 the difference $I_D(Q) = I_{60K}(Q) - I_{240K}(Q)$, which is a measure of the spatial distribution of the dynamic fluctuations of the protons, is plotted vs Q. After

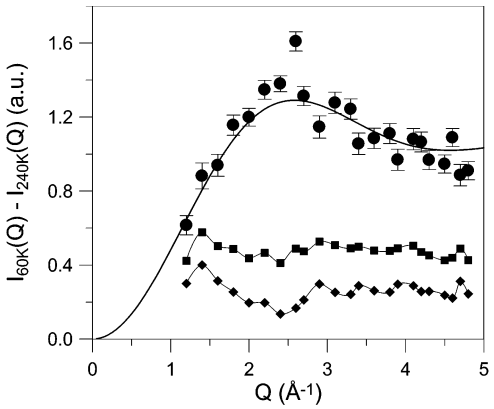

Figure 6. Difference between the elastic intensity at 60 and 240 K (full circles) plotted vs Q, with the model function $I_D(Q)$ (see eq 6) shown as a full line. The separate values of $I_{60K}(Q)$ and $I_{240K}(Q)$ are also given as squares and diamonds, respectively, rescaled by a factor of 0.2.

rescaling, the two corresponding elastic $I(Q)$ curves are also therein reported; overlapping of Bragg peaks is evident, owing to the comparably poor Q resolution of the spectrometer with respect to a diffractometer. Below 100 K the dynamics is very slow and the protons are fairly well localized, whereas above 200 K they are delocalized between the six equivalent positions observed by the neutron Bragg diffraction experiment.[6] Considering the structure of the hydronium ion therein determined (Figure 1), two possible jumping paths can be identified between the six equivalent positions, assuming that a jump can occur between occupied and unoccupied position at the rate given by the inverse of the quasi-elastic peak width. The two distances are $R_1 = 1.58$ Å and $R_2 = 2.10$ Å, with weights 2 and 1, respectively. By assuming that this confined jumping mechanism holds, and that the present sample is a "good" powder, we can represent $I_D(Q)$ as follows:[14]

$$I_D(Q) = K\left\{2\left[1 - \frac{\sin(QR_1)}{QR_1}\right] + 1 - \frac{\sin(QR_2)}{QR_2}\right\} \qquad (6)$$

where K is a normalization constant. The curve of eq 6 is also shown in Figure 6, where it can be seen to agree excellently with the experimental results. Therefore, we can conclude that the dynamics observed at high temperature is dominated by the proton jump between the different configurations of the H_3O^+ ion. A more extended investigation of the quasi-elastic peak vs temperature would confirm that this is a thermally activated process and would allow one to determine the corresponding activation energy.

4. Conclusions

On the basis of all results obtained, the complex disorder of the hydronium ion in $(H_3O)Zr_2(PO_4)_3$ is shown to have a dynamical character, leading to the following conclusions. First, the monoclinic structure of the LT phase is characterized by a distribution of the H atoms, which cannot be completely static, as a proton dynamics slower than 100 ps is still present. Therefore, the residual disorder observed in the diffraction study,[6] with one of the three H atoms of the hydronium ion distributed over two sites with 2/3 and 1/3 probabilities, is proved to have an important dynamical component. Further, the proton motion is clearly shown to be localized by the absence

of any Q dependence of the width of the quasi-elastic peak. The space range of this dynamics could be fully determined by exploring larger Q values, so as to confirm or not that only two sites are involved in the motion, as the site-to-site distances would be different according to the number of sites. A very detailed temperature scan would also be needed, to discriminate between two possible origins of the motion: either a classical thermally activated jump between different sites, with an Arrhenius-like T dependence of the quasi-elastic peak width, or a quantum-mechanical tunneling, which can be observed at low temperature only with negligible thermal dependence.

The second conclusion concerns the behavior of the HT disordered phase. In this case the proton dynamics is much faster, and it becomes faster and faster on increasing the temperature. The experimental energy range of this high-temperature motion is in perfect agreement with the interpretation of the motion as a classical jump between occupied and empty sites around the oxygen atom of the H_3O^+ ion. Therefore, the motion we have observed has no relationship with a diffusion-like proton transport, which would occur on a different time and distance scale. This confirms, on a direct dynamical basis, the mechanism proposed in the previous study[6] for proton mobility in $(H_3O)Zr_2(PO_4)_3$ Nasicon, which relies on thermally activated hopping with no diffusion processes.

References and Notes

(1) Catti, M.; Stramare, S.; Ibberson, R. *Solid State Ionics* **1999**, *123*, 173.
(2) Catti, M.; Comotti, A.; Di Blas, S. *Chem. Mater.* **2003**, *15*, 1628.
(3) Subramanian, M. A.; Roberts, B. D.; Clearfield, A. *Mater. Res. Bull.* **1984**, *19*, 1471.
(4) Canaday, J. D.; Chehab, S. F.; Kuriakose, A. K.; Ahmad, A.; Wheat, T. A. *Solid State Ionics* **1991**, *48*, 113.
(5) Rudolf, P. R.; Subramanian, M. A.; Clearfield, A. *Solid State Ionics* **1985**, *17*, 337.
(6) Catti, M.; Ibberson, R. M. *J. Phys. Chem. B* **2002**, *106*, 11916.
(7) Zhu, L.; Seff, K.; Olson, D. H.; Cohen, B. J.; Von Dreele, R. B. *J. Phys. Chem. B* **1999**, *103*, 10365.
(8) Smith, L.; Cheetham, A. K.; Morris, R. E.; Marchese, L.; Thomas, J. M.; Wright, P. A.; Chen, J. *Science* **1996**, *271*, 799.
(9) Ikeda, S.; Fillaux, F. *Phys. Rev. B* **1999**, *59*, 4134.
(10) Fillaux, F.; Cousson, A.; Keen, D. *Phys. Rev. B* **2003**, *67*, 054301.
(11) Reiter, G. F.; Mayers, J.; Platzman, P. *Phys. Rev. Lett.* **2002**, *89*, 135505.
(12) Ohta, M.; Ono, A.; Okamura. F. P.; *J. Mater. Sci. Lett.* **1987**, 6, 583.
(13) Butler, M. A.; Biefeld, R. M. *Phys. Rev. B* **1979**, *19*, 5455.
(14) Bée, M. *Quasielastic Neutron Scattering*; Adam Hilger: Bristol and Philadelphia, 1988; pp 189−192.